

STRANGENESS PRODUCTION IN HEAVY ION COLLISIONS AT RELATIVISTIC ENERGIES*

OANA RISTEA, A. JIPA, C. RISTEA, C. BEȘLIU, ȘTEFANIA VELICA

University of Bucharest, Faculty of Physics, Romania
E-mail: oana@brahms.fizica.unibuc.ro

Received July 29, 2011

Abstract. We present measurements of charged kaon production at different rapidities from Au-Au collisions at $\sqrt{s_{NN}} = 200$ GeV. Effective temperatures and rapidity densities for positive and negative kaons are investigated as a function of collision energy and rapidity. The results are also compared to previous measurements at various energies.

Key words: heavy ion collisions, quark-gluon plasma, strangeness enhancement.

1. INTRODUCTION

Heavy-ion collisions at high energies offer a unique opportunity to probe highly excited dense nuclear matter with properties very different from that of a hadron gas or ordinary nuclear matter in the laboratory [1]. Within the past several years there was an extraordinary progress on various aspects of elementary particle properties and related phenomena such as heavy ion collisions at relativistic energies [2]. One of the proposed quark-gluon plasma (QGP) signals is the increased strangeness production compared to that of a hadron gas [3]. Strange particles are of particular interest since all strange hadrons must be formed in the produced matter. Other processes can also enhance strangeness production [4] and, therefore, elementary p-p collisions, where QGP formation is unlikely, are important as a reference. An enhanced strangeness production in heavy ion collisions relative to p-p at the same energy could signal QGP formation.

2. EXPERIMENTAL SET-UP

BRAHMS [5] is one of the four experiments from the Relativistic Heavy Ion Collider (RHIC) [6]. The BRAHMS experiment consists of two movable

* Paper presented at the Annual Scientific Session of Faculty of Physics, University of Bucharest, June 17, 2011, Bucharest-Magurele, Romania.

spectrometers and a set of detectors used to determine global features of the collision such as the overall charged particle multiplicity, the collision vertex and the centrality of the collision. Mid-Rapidity Spectrometer (MRS), which operates in the polar angle interval from 90° to 30° , is composed of a single dipole magnet placed between two Time Projection Chambers (TPC) and a Time-of-Flight (TOF) detector for particle identification. Forward Spectrometer (FS), which operates in the angular range of $15^\circ < \theta < 2.3^\circ$ (θ is the polar angle with respect to the beam direction), has two TPCs, three Drift Chambers and four dipole magnets. Particle identification in the FS is provided by TOF measurements in two separate hodoscopes (H1 and H2) and/or using a Ring Imaging Cherenkov detector (RICH) located at the end of the spectrometer. The mid-rapidity arm is capable of separating pions from Kaons up to 2 GeV/c and charged kaons from protons/antiprotons up to 3 GeV/c, while the forward arm can identify particles up to 35–40 GeV/c by using the Cherenkov ring detector (RICH).

3. RESULTS AND DISCUSSION

The transverse momentum spectra for charged kaons measured by BRAHMS experiment in Au-Au collisions at $\sqrt{s_{NN}} = 200$ GeV are fitted in order to extract the effective temperatures (inverse slope parameters):

$$\frac{1}{2\pi p_T} \frac{d^2N}{dp_T dy} = \frac{dN/dy}{2\pi T(T+m)} \exp\left(-\frac{\sqrt{m^2 + p_T^2}}{T}\right), \quad (1)$$

where dN/dy is the rapidity density, T is the effective temperature, m is the rest mass of the particle and p_T is the transverse momentum. This fit formula gives a good description of kaonic spectra shapes as illustrated in Fig. 1.

The inverse slope parameters for K^+ and K^- as a function of rapidity are shown in Fig. 2. The kaon slopes show strong rapidity dependence. The mid-rapidity values ($0 \leq y \leq 1$) are around ~ 310 MeV, start decreasing as $y \geq 2$ and finally reach values as low as ~ 230 MeV at $y \sim 3.5$. The decrease is $\sim 30\%$ from mid-rapidity to the highest rapidity measured and may be interpreted as due to the decrease of collective transverse flow as the rapidity increases. The inverse slopes obtained at forward rapidities are higher for positive kaons than for the negative kaons. Also, remarkable is the similarity between spectral features of K^+ and K^- particles and may indicate that sources of particles and antiparticles have similar characteristics at all rapidities covered by this analysis.

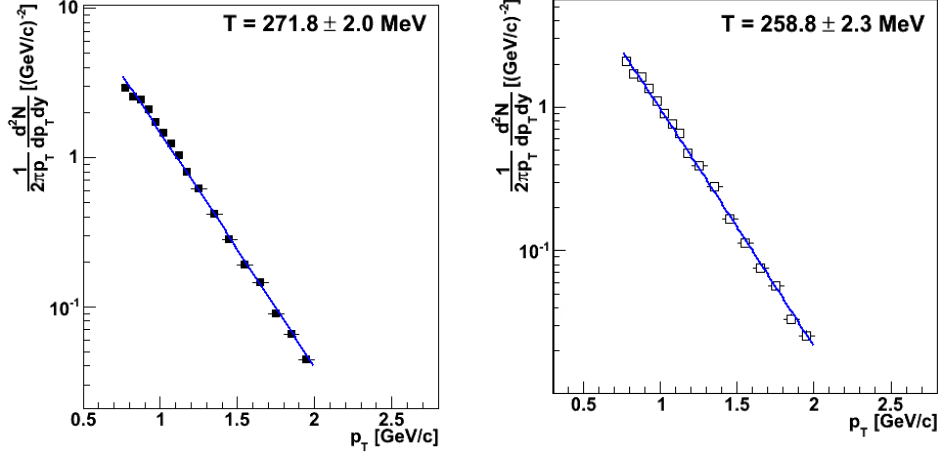


Fig. 1 – Transverse momentum spectra for K^+ (left) and K^- (right) produced in central 0–10% Au-Au collisions at 200 GeV at rapidity $y = 3.1$. Blue lines represent the fit to the spectra with formula (1) in order to obtain the inverse slope parameters.

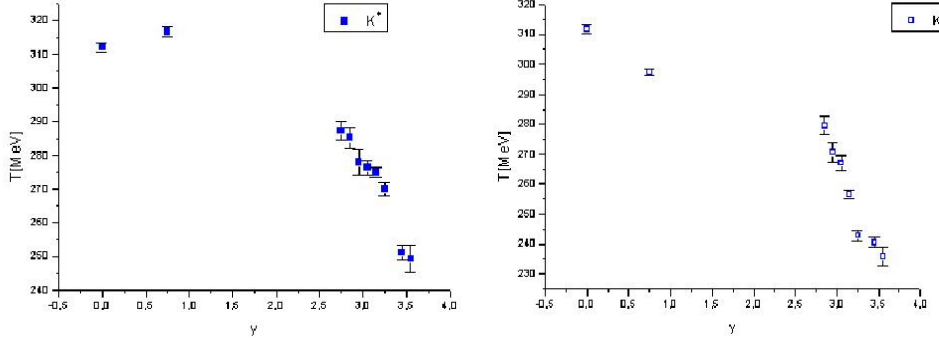


Fig. 2 – The inverse slope parameters for K^+ (left) and K^- (right) from central 0–10% Au-Au collisions at 200 GeV as a function of rapidity.

At a given rapidity, the kaon transverse momentum spectrum is measured in a limited p_T range. To extract the rapidity density, dN/dy , it is necessary to extrapolate from the p_T range where spectrum is measured to the full interval ($0 < p_T < \infty$). This extrapolation is accomplished by using the fit function (1), which describes well the measured data points. Then, the total rapidity density is calculated by taking the sum of the yield from the data and the yield from the functional form in the unmeasured p_T region.

The dN/dy values at midrapidity for different collision systems at various energies are summarized in Table 1. They are plotted in Fig. 3 as a function of collision energy, $\sqrt{s_{NN}}$. The heavy ion data at lower energies and the p-p data are

taken from Refs. [7–9]. The values indicate that dN/dy increases for K^+ and K^- species produced in heavy ion collisions with energy and saturates around RHIC top energy. The rapidity densities for negative kaons are systematically lower than rapidity densities for positive kaons at all rapidities.

At another energy (for example, at 17.3 GeV), the strangeness production is system-size dependent as a consequence of the changes in reaction mechanism due to the transition from an isolated N-N interaction to the A-A situation, where nucleons undergo subsequent collisions within short time intervals and close in space. The data obtained in symmetric nucleus-nucleus collisions show a rise of the strangeness content in the produced hadrons with increasing size of the colliding systems.

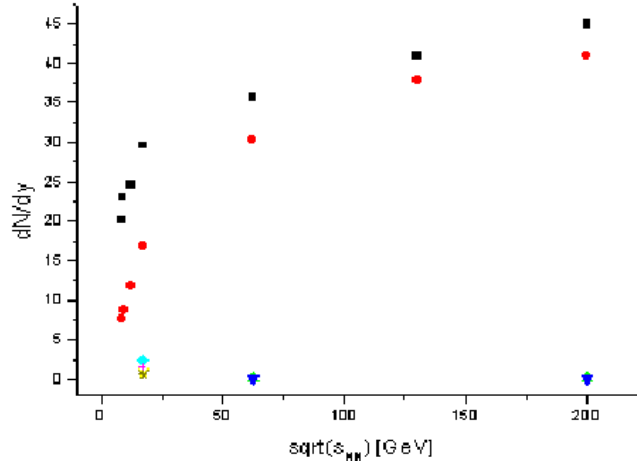


Fig. 3 – The dN/dy for K^+ (black points) and K^- (red points) at midrapidity, for central 0–10% Au-Au collisions at 200 GeV (this analysis) compared to previous results from SPS and RHIC.

The blue points from 62.4 GeV and 200 GeV are from p+p collisions. The blue-magenta-brown points at 17.3 GeV are from C+C and Si+Si collisions.

Table 1

The collisions, energy in the center of mass system, rapidity densities for positive kaons and negative kaons and K^-/K^+ ratio

| Reaction | $\sqrt{s_{NN}}$ [GeV] | $dN/dy(K^+)$ | $dN/dy(K^-)$ | K^-/K^+ |
|----------|-----------------------|--------------|--------------|-----------|
| Pb+Pb | 8.8 | 20.1 | 7.6 | 0.37 |
| Au+Au | 9.2 | 23.0 | 8.7 | 0.38 |
| Pb+Pb | 12.3 | 24.6 | 11.7 | 0.46 |
| C+C | 17.3 | 2.6 | 1.5 | 0.57 |
| Si+Si | 17.3 | 7.5 | 4.5 | 0.59 |
| Pb+Pb | 17.3 | 29.6 | 16.8 | 0.57 |
| Au+Au | 62.4 | 35.6 | 30.4 | 0.85 |
| Au+Au | 130 | 41.0 | 37.9 | 0.92 |
| Au+Au | 200 | 47.0 | 44.1 | 0.94 |

There are two possible kaon production mechanisms: pair production of K^+ and K^- and associated production of $K^+(K^-)$ with a hyperon (antihyperon). To disentangle between the relative contributions from these two mechanisms, Fig. 4 shows the K^-/K^+ ratio as a function of collision energy, $\sqrt{s_{NN}}$ in heavy ion collisions.

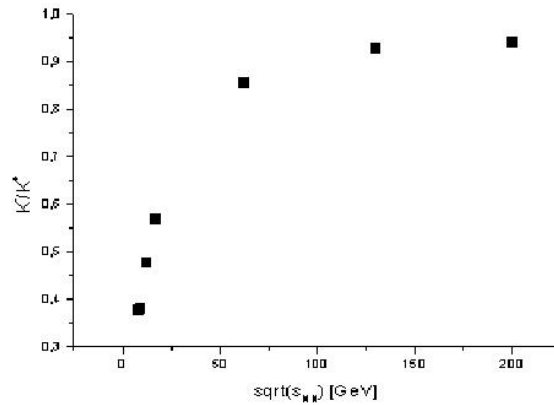


Fig. 4 – The K^-/K^+ at midrapidity, for central 0–10% Au-Au collisions at 200 GeV compared to previous results from SPS and RHIC.

The ratio increases with energy. It reflects interplay between the associated production of K^+ at low energy (sensitive with baryon density of the medium, which is higher at lower energies) and the dominance of equal K^+ and K^- production *via* either pair production of K^+K^- or associated production of $K^+(K^-)$ with hyperon (antihyperon) at high energies.

4. CONCLUSIONS

In summary, we have measured the transverse momentum spectra of charged kaons in central Au-Au collisions at 200 GeV. The inverse slope parameters for charged kaons show a decrease at forward rapidity and may be interpreted as a consequence of the smaller transverse collective flow from less dense local system. The rapidity densities for charged kaons increase with collision energy. The K^-/K^+ ratio reflects interplay between the decreasing importance of associated production and an increasing contribution from pair production of kaons with increasing collision energy.

Acknowledgements. The work of Oana Ristea and Catalin Ristea was supported by the strategic grant POSDRU/89/1.5/S/58852, Project „Postdoctoral programme for training scientific researchers”, co-financed by the European Social Found within the Sectorial Operational Program Human Resources Development 2007-2013. The work of Stefania Velica was supported by the

Project POSDRU/6/1.5/S/10, “Projected development and performance in doctoral research of interdisciplinary type“. We thank the BRAHMS Collaboration for their excellent and dedicated work to acquire and process the unique experimental data and their support to our group.

REFERENCES

1. Al. Jipa, C. Besliu, *Elemente de Fizică Nucleară Relativistă. Note de curs*, Editura Universității București, 2002;
E. Shuryak, Nucl.Phys.Proc.Suppl., **195**, 111 (2009);
J.P. Blaizot, <http://arxiv.org/abs/hep-ph/01071311>;
J. Rafelski, J. Letessier, Eur.Phys., J **A29**, 107 (2006).
2. M. Petrovici *et al.*, Rom J. Phys., **56**, 654 (2011);
M. Petris *et al.*, Rom J. Phys., **56**, 349 (2011);
A. Saftoiu *et al.*, Rom. J. Phys., **56**, 664 (2011);
A. M. Apostu *et al.*, Rom. Rep. Phys., **63**, 220 (2011);
G. Toma *et al.*, Rom. Rep. Phys., **63**, 383 (2011);
B. Mitrica *et al.*, Rom. Rep. Phys., **62**, 750 (2010);
M. I. Cherciu and A. Jipa, Rom. Rep. Phys., **62**, 731 (2010);
M. Petris *et al.*, Rom J. Phys., **55**, 324 (2010).
3. J. Rafelski, Phys. Rept., **88**, 331 (1982);
P. Koch, B. Muller and J. Rafelski, Phys. Rept., **142**, 167 (1986).
4. H. Sorge, Phys. Rev., C **52**, 3291 (1995).
5. BRAHMS Collaboration, Nucl. Instr. Meth., **A499**, 437 (2003).
6. *** www.bnl.gov/RHIC/
7. NA49 Collaboration, Phys. Rev. Lett., **94**, 052301 (2005); <http://arxiv.org/abs/nucl-ex/0205002> ;
<http://arxiv.org/abs/nucl-ex/0806.1937>
8. BRAHMS Collaboration, Phys. Lett., B **687**, 36–41 (2010).
9. PHENIX Collaboration, <http://arxiv.org/abs/1102.0753>